Human Molecular Genetics, 2007, Vol. 16, No. 9 ***1078–1090***
doi:10.1093/hmg/ddm057
Advance Access published on March 14, 2007

Hsp27 overexpression in the R6/2 mouse model of Huntington's disease: chronic neurodegeneration does not induce Hsp27 activation

Alexandra Zourlidou[1], Tali Gidalevitz[2], Mark Kristiansen[3], Christian Landles[1], Ben Woodman[1], Dominic J. Wells[4], David S. Latchman[5], Jackie de Belleroche[4], Sarah J. Tabrizi[3], Richard I. Morimoto[2] and Gillian P. Bates[1,*]

[1]Department of Medical and Molecular Genetics, King's College London, School of Medicine, London SE1 9RT, UK, [2]Department of Biochemistry, Molecular Biology and Cell Biology, Northwestern University, Evanston, IL 60208, USA, [3]Department of Neurodegenerative Disease, MRC Prion Unit, Institute of Neurology, Queen Square, London WC1 N 3BG, UK, [4]Division of Neuroscience and Psychological Medicine, Faculty of Medicine, Imperial College London, Charing Cross Hospital, London W6 8RF, UK and [5]Birkbeck College, University of London, Malet Street, London WC1E 7HX, UK

Received November 10, 2006; Revised and Accepted March 2, 2007

Huntington's disease (HD) is caused by an expanded polyglutamine tract in the huntingtin protein. Mitochondrial dysfunction and free radical damage occur in both R6/2 mice and HD patient brains and might play a role in disease pathogenesis. In cell culture systems, heat-shock protein 27 (Hsp27), a small molecular chaperone, suppresses mutant huntingtin-induced reactive oxygen species formation and cell death. To investigate this *in vivo*, we conducted an extensive phenotypic characterization of mice arising from a cross between R6/2 mice and Hsp27 transgenic mice but did not observe an improvement of the R6/2 phenotype. Hsp27 overexpression had no effect in reducing oxidative stress in the R6/2 brain, assessed by measuring striatal aconitase activity and protein carbonylation levels. Native protein gel analysis revealed that transgenic Hsp27 forms active, large oligomeric species in heat-shocked brain lysates, demonstrating that it is efficiently activated upon stress. In contrast, Hsp27 in double transgenic brains exists predominantly as a low molecular weight, inactive species. This suggests that Hsp27, which is otherwise activatable upon heat shock, remains inactive in the R6/2 model of chronic neurodegeneration. Hsp27 transgenics had been previously shown to be protected from acute stresses such as kainate administration, ischemia/reperfusion heart injury and neonatal nerve injury. Our study is the first to suggest a differential modulation of Hsp27 activation *in vivo* and, importantly, it illustrates the diverse effect of Hsp27 on acute versus chronic models of disease.

INTRODUCTION

Huntington's disease (HD) is an autosomal dominant late-onset progressive neurodegenerative disorder (1). Onset is generally in mid-life, and patients develop psychiatric disturbances, impairment of motor coordination, including involuntary choreic movements, and later bradykinesia and cognitive decline. It is a devastating disorder for which the duration is 15–20 years, and there is no effective therapy. The HD mutation is an expanded CAG/polyglutamine (polyQ) repeat. Unaffected individuals have $(CAG)_{6-35}$ repeats; $(CAG)_{36-39}$ show incomplete penetrance, whereas repeats of 40 and more will always cause disease within a normal lifespan. CAG repeats of ~60 and above cause the childhood or adolescent form of the disease. Neuropathologically, the disease is characterized by neuronal cell loss in the striatum, cortex and other

*To whom correspondence should be addressed at: Department of Medical and Molecular Genetics, King's College London, School of Medicine, 8th floor Guy's Tower, Guy's Hospital, London SE1 9RT, UK. Tel: +44 2071883722; Fax: +44 2071882585; Email: gillian.bates@genetics.kcl.ac.uk

brain regions, and recent neuroimaging studies suggest that a more generalized brain atrophy occurs in the early stages of disease (2). Polyglutamine aggregates have been detected within the nucleus and cytoplasm (3,4).

The R6/2 mouse expresses exon 1 of the human HD gene with more than 150 CAG repeats (5). It has a rapid and reproducible phenotype progression that recapitulates many features of the human disease. Motor and cognitive abnormalities can be detected before 6 weeks of age (6,7), and mice are rarely kept beyond 15 weeks. Polyglutamine aggregates are clearly apparent in some brain regions from 3 to 4 weeks of age (8,9) and have been described at even earlier stages (10), and striatal cell loss has been documented at later stages (10). This suggests that the mouse phenotype is predominantly caused by neuronal dysfunction. In addition, phenotypes identified in the R6/2 mouse have subsequently been shown to be present in the human disease. These include the down-regulation of neurotransmitter receptors (11,12), the loss of orexin neurons in the hypothalamus (13) and muscle pathology (14).

Multiple mechanisms have been proposed to account for the neuronal dysfunction caused by mutant huntingtin. For example, similar mitochondrial abnormalities and evidence of oxidative damage have been reported in patient (15) and R6/2 brains (16). Strikingly, heat-shock proteins (Hsps) have been shown to be protective in many of the pathways that are implicated in HD, including native and non-native protein folding, cytoprotection from various stresses such as oxidative stress and modulation of cell death and survival pathways. Hence, chaperones comprise eligible candidates for neuroprotection in HD (17,18) and their potential has been evaluated in *in vitro* (19), yeast (20), *Caenorhabditis elegans* (21), *Drosophila* (22,23), mammalian cells (24–27) and *in vivo* models of HD (28–31), with varying degrees of success. For instance, Hsp70 mice were crossed to R6/2, resulting in only modest effects on disease progression (29) or no alteration of the phenotype apart from a delay in aggregate formation by a week (28). More recently, yeast Hsp104 transgenic mice were crossed with N171-82Q mice (31), but again there was no amelioration of the disease phenotype (weight loss, motor impairment), apart from aggregate reduction in the piriform cortex and increased survival.

In an elegant study by Wyttenbach *et al.* (27), transient overexpression of Hsp27 was shown to suppress polyQ-mediated cell death in an *in vitro* cellular model of HD. Mutant huntingtin caused increased levels of reactive oxygen species (ROS) in both neuronal and non-neuronal cells, leading to cell death. Overexpression of Hsp27 significantly reduced ROS content, suggesting that Hsp27 strongly protects cells against oxidative stress. This protection was regulated by the phosphorylation status of Hsp27 and was independent of its ability to bind to cytochrome *c*. Notably, and in contrast to Hsp40 and Hsp70, Hsp27 suppressed polyQ death but not polyQ aggregation.

There are many studies that have detected oxidative stress and mitochondrial impairment in HD (32–34). In particular, increased oxidative damage of DNA has been identified in the caudate and frontal cortex of HD post-mortem brains (35), reduced complex II/III activity in the putamen and caudate nucleus and complex IV activity in the putamen (15,35–37). HD muscle biopsies have reduced complex I activity in some patients (38), but no such alterations in oxidative phosphorylation activities were detected in HD platelets or fibroblasts (15,37). Mitochondrial aconitase activity was greatly decreased in patients' caudate (92% reduction), cerebral cortex (48% reduction) and putamen (73% reduction), but not in the cerebellum (15). Evidence for mitochondrial dysfunction, free radical damage (16,39) and increased oxidative DNA damage (40) have also been reported in the R6/2 mouse.

In this study, we asked whether global overexpression of Hsp27 in R6/2 mice could ameliorate the well-established R6/2 phenotype and alter aspects of the disease pathology at the biochemical level *in vivo*. In contrast to the *in vitro* work, our results indicated that constitutive ubiquitous Hsp27 overexpression does not modify the disease progression or biochemical markers *in vivo*. Native protein gel analysis suggests that the stress accompanying chronic neurodegeneration fails to activate the overexpressed transgenic Hsp27 in the mouse. We suggest that inducible systems are required to properly test the therapeutic potential of chaperone induction in a mammalian system.

RESULTS

The Hsp27 transgenic mice (tgHsp27) express human Hsp27 under the control of the chicken-β-actin promoter and have been described previously (41). They have been used to show that Hsp27 overexpression is neuroprotective against kainate-induced neuronal loss in a model of epilepsy (41), cytoprotective in the mouse heart against ischaemia reperfusion injury (42) and protects motor neurons in a model of nerve injury in which Hsp27 also preserves muscle function (43). We set out to use this model to determine whether overexpression of Hsp27 might also be protective in the R6/2 mouse model of HD. TgHsp27 line 18 was chosen for this purpose, because it had been shown to express Hsp27 in neuronal cell bodies throughout the brain, particularly in the hippocampus, cerebral cortex, cerebellum, striatum, thalamus and subventricular nuclei, as well as in fibrous networks and glial cells (41).

Overexpression of Hsp27 does not modify the R6/2 behavioural phenotype

We have previously established a set of quantitative tests with which to monitor the progressive behavioural phenotype in the R6/2 mice (44,45). To generate mice for this analysis, male R6/2 mice were bred with female tgHsp27 mice to produce 15 female mice from each genotype (R6/2, Hsp27, R6/2xHsp27 double transgenics and wild-type), which were born over a period of 2 days. The CAG repeat size was well matched: 220 ± 0.6 for the R6/2 mice and 217 ± 1.8 for the double transgenics. Weight gain, RotaRod performance, grip strength and exploratory activity were monitored at the same day/time of the week from weeks 4 to 15, when the experiment was terminated.

Mice were weighed weekly, except during the weeks of RotaRod trials when they were weighed on the first and last

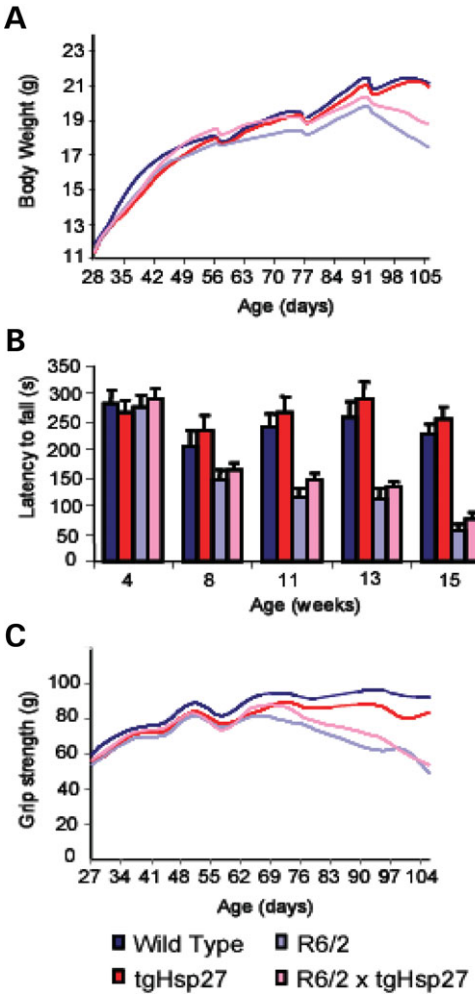

Figure 1. Hsp27 overexpression does not alter the behavioural phenotype of the R6/2 mice. (**A**) Weight loss is not ameliorated in R6/2 mice by constitutive expression of Hsp27 ($P = 0.2$). Double transgenic and R6/2 mice lose weight from 90 days of age. The periodic sharp drop in weight corresponds to weight loss during the RotaRod trials at 4, 8, 11 and 13 weeks. (**B**) There is a similar decline in RotaRod performance for both R6/2 and double transgenic mice with respect to time ($P = 0.65$) and ($P = 0.83$) genotype. Error bars represent standard errors of the mean. (**C**) Grip strength in the double transgenics is not significantly different when compared with R6/2 mice over time ($P = 0.80$) or with respect to genotype ($P = 0.07$). All data were analysed by GLM ANOVA ($n = 15$ female mice per genotype for all tests).

days of RotaRod assessment. As expected, R6/2 mice lost weight from 90 days when compared with wild-type (wt) animals (Fig. 1A) ($F_{(4,\ 214)} = 18.04$, $P < 0.001$). There was no difference in the rate of weight gain between tgHsp27 and wt mice ($F_{(4,\ 214)} = 1.70$, $P = 0.16$). Hsp27 overexpression did not attenuate the R6/2 weight loss as they grew older ($F_{(4,\ 214)} = 0.40$, $P = 0.8$), and double transgenics are not significantly different from R6/2 with respect to weight gain ($F_{(1,56)} = 1.65$, $P = 0.2$). Therefore, overexpression of Hsp27 does not improve weight loss in the R6/2 mice.

RotaRod performance is a sensitive indicator of balance and motor coordination, which has been repeatedly shown to decline in R6/2 mice. Using this test, R6/2 and double transgenic mice perform similarly over time, whereas the performance of Hsp27 mice is equivalent to wt mice (Fig. 1B). Consistent with previous results, there was a significant difference in RotaRod performance between R6/2 and wt mice over time ($F_{(3,\ 153)} = 33$, $P < 0.001$). However, there is no difference between double transgenics and R6/2 performance over time ($F_{(3,\ 153)} = 0.53$, $P = 0.65$) or with respect to genotype ($F_{(1,\ 550)} = 0.05$, $P = 0.83$).

Forelimb grip strength was also assessed weekly from week 4 to week 15 (Fig. 1C). R6/2 performed significantly worse than wt over the time ($F_{(6,\ 312)} = 18.5$, $P < 0.001$), whereas tgHsp27 mice had a grip strength comparable to wt over the course of the experiment ($F_{(6,\ 312)} = 0.7$, $P = 0.64$). Overexpression of Hsp27 did not improve R6/2 grip strength, as the double transgenics performed similarly when compared with R6/2 both with respect to time ($F_{(6,\ 312)} = 0.5$, $P = 0.8$) and genotype ($F_{(1,\ 56)} = 3.5$, $P = 0.7$).

Exploratory activity was also assessed weekly from week 4 to week 15 as described previously (45) and analysed by repeated measures general linear model (GLM) ANOVA at each time point. Mice were assessed for a period of 60 min for total activity, mobility, rearing and centre rearing (Fig. 2, examples given for weeks 6 and 13) and *P*-values obtained are summarized in Table 1. As seen in Fig. 2, mice of all genotypes exhibit most activity during the first few minutes of the assessment period, which then decreased dramatically over the hour (time). R6/2 mice show a progressive hypoactivity relative to wt mice (Fig. 2 and Table 1: R6/2) and a progressive change in the pattern of activity (note the slope of the curve in Fig. 2) when compared with wt mice (R6/2 × time). TgHsp27 mice display an overall hypoactivity relative to wt mice (tgHsp27), but in this case, the pattern of the activity is not altered (tgHsp27 × time). There was no overall improvement in R6/2 hypoactivity by overexpression of Hsp27 (R6/2 × tgHSp27) and neither was the R6/2 pattern of hypoactivity changed (R6/2 × tgHsp27 × time). Therefore, the decrease in the activity of the double transgenic mice when compared with R6/2 mice over the course of the experiment (Fig. 2) is the consequence of an additive effect and not a genotype interaction. In summary, tgHsp27 mice display an overall hypoactivity when compared with wt mice, and overexpression of Hsp27 does not improve R6/2 hypoactivity.

The R6/2 transgene does not alter Hsp27 protein levels in the double transgenic mice

Transcriptional dysregulation is a well-described aspect of the HD pathogenesis in both the R6/2 mouse model (46,47) and HD patient brains (48). In order to ensure that the Hsp27 transgene had not been down-regulated in the double transgenic mice, we measured the levels of Hsp27 and endogenous Hsp25 in all four genotypes. Western blotting was performed on week 15 brains (four males and four females per genotype). This confirmed that there was no difference in the level of the Hsp27 protein in the double transgenic mice at the termination of the experiment (Fig. 3A). For quantification purposes, an antibody that was raised against mouse Hsp25 and also recognizes human Hsp27 was used and the blots were analysed using a phosphorimager. Levels of Hsp27 were determined in relation to the endogenous mouse Hsp25, which was

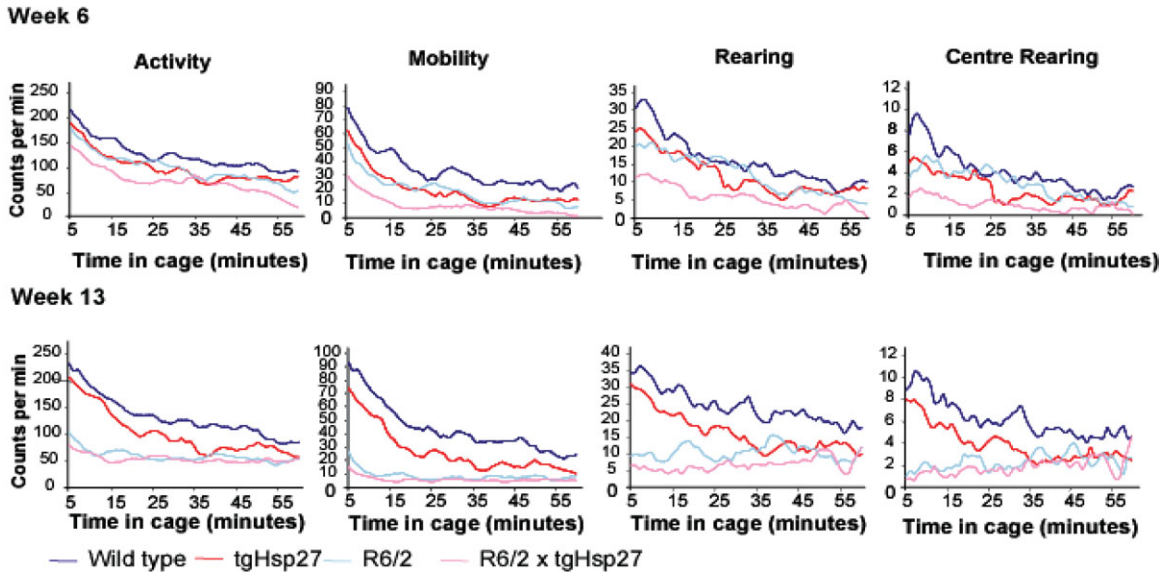

Figure 2. The progressive hypoactivity and abnormal exploratory behaviour of the R6/2 mice is not improved by Hsp27 overexpression. Four measures of the exploratory activity of the mice were analysed weekly between week 4 and week 15. Representative graphs display 5 min moving averages and show total activity, mobility, rearing and centre rearing at weeks 6 and 13. Mice of all genotypes are most active when first placed in the activity cage, and this decreases over the 60 min assessment period. At 6 weeks of age, R6/2 mice already show a significant difference when compared with wt with respect to overall activity and the pattern of activity (slope of the graph) (Table 1: R6/2). TgHsp27 mice also shows an overall hypoactivity by this age (Table 1: TgHsp27), but the temporal pattern of this remains unaltered (Table 1: TgHsp27 × time). At 6 weeks, the double transgenic mice are hypoactive with respect to R6/2. This effect is additive, and there is no synergistic interaction between R6/2 and Hsp27 either overall or with time (Table 1). The phenotype progresses with the age of the mice, and at 13 weeks of age, the effects observed at 6 weeks are exacerbated. By 13 weeks, R6/2 and the double transgenic mice are displaying similar levels of hypoactivity; $n = 15$ mice per genotype.

expressed at the same level in all four genotypes. Hsp27 expression was ~12-fold higher than Hsp25 (Fig. 3B), but there were small variations in Hsp27 expression level between animals (Fig. 3B). Western blots using enhanced chemiluminescence as a detection method, instead of a fluorescent secondary antibody, showed similar high expression levels (data not shown).

Hsp27 overexpression does not ameliorate markers of oxidative stress in R6/2 mouse brains

As overexpression of Hsp27 had reduced levels of oxidative stress in a cell culture model of HD (27), we next determined whether Hsp27 might have had a similar effect in the double transgenic mouse brains. Loss in mitochondrial aconitase activity is used as a biomarker of oxidative damage due to the susceptibility of the enzyme's $[4Fe\text{-}4S]^{2+}$ cluster to oxidative damage by peroxynitrite and superoxide radicals and had been previously shown to be decreased in the striata from R6/2 mice at 12 weeks of age (16). Therefore, this enzyme activity was measured in the striata of wt, R6/2, tgHsp27 and double transgenic mice at 15 weeks of age upon termination of the behavioural experiments ($n = 15$ per genotype). This confirmed that the activity of mitochondrial aconitase is decreased in the R6/2 striatum when compared with wt ($P = 0.013$) and determined that it is also decreased in the striata of the double transgenic mice ($P = 0.003$) (Fig. 4A). There was no improvement in aconitase activity in the double transgenics when compared with R6/2 ($P = 0.2$).

To further investigate the potential of Hsp27 to modulate oxidative stress *in vivo*, we used Oxyblots to determine first, whether protein carbonylation levels were altered in R6/2 brains when compared with wt at 8 and 13 weeks of age and secondly, whether this could be attenuated by Hsp27 overexpression. Carbonyl groups are introduced into proteins by oxidative reactions of nitrogen oxides or by metal-catalysed oxidation in the tissue and have been measured using Oxyblots in various studies (49–51). An antibody against 2,4--dinitrophenylhydrazone (DNP-hydrazone) was used to detect protein carbonyls, which were derivatized in the samples by reaction with 2,4-dinitrophenylhydrazine prior to polyacrylamide gel electrophoresis and immunobloting (Fig. 4B). The molecular weight protein standard also served as a positive control for DNP-hydrazone detection, since it was composed of five different proteins with DNP residues. Lane 2 contains a non-derivatized protein sample of R6/2 brain, which served as a negative control (Fig. 4B). Figure 4 also illustrates the change in protein carbonyls relative to wt levels in brains from 8-week-old ($n = 4$) (Fig. 4C) and 13-week-old ($n = 6$) mice (Fig. 4D). There is a significant 2-fold difference in protein carbonyls between R6/2 and wt brain at 13 weeks of age ($P < 0.01$), but there is no difference at 8 weeks. However, at 13 weeks, there is no significant difference in protein carbonyl levels when comparing double transgenics to R6/2 ($P < 0.01$). Carbonyl levels in double transgenics are also ~2-fold higher than the levels in wt or tgHsp27 mice (Fig. 4D). Therefore, overexpression of Hsp27 has not suppressed the oxidative damage caused by the ROS

Table 1. Statistical analysis of activity measurements

	Week	Activity	Mobility	Rearing	Centre rearing
Time	4	$<0.001^{***}$	$<0.001^{***}$	$<0.001^{***}$	$<0.001^{***}$
	5	$<0.001^{***}$	$<0.001^{***}$	$<0.001^{***}$	$<0.001^{***}$
	6	$<0.001^{***}$	$<0.001^{***}$	$<0.001^{***}$	$<0.001^{***}$
	7	$<0.001^{***}$	$<0.001^{***}$	$<0.001^{***}$	$<0.001^{***}$
	8	$<0.001^{***}$	$<0.001^{***}$	$<0.001^{***}$	0.001^{**}
	9	$<0.001^{***}$	$<0.001^{***}$	$<0.001^{***}$	$<0.001^{***}$
	10	$<0.001^{***}$	$<0.001^{***}$	$<0.001^{***}$	$<0.001^{***}$
	11	$<0.001^{***}$	$<0.001^{***}$	$<0.001^{***}$	$<0.001^{***}$
	13	$<0.001^{***}$	$<0.001^{***}$	$<0.001^{***}$	0.297
	14	$<0.001^{***}$	$<0.001^{***}$	$<0.001^{***}$	$<0.001^{***}$
	15	$<0.001^{***}$	$<0.001^{***}$	$<0.001^{***}$	$<0.001^{***}$
R6/2	4	0.394	0.223	0.017^{*}	0.017^{*}
	5	0.679	0.035^{*}	0.054	0.177
	6	0.008^{**}	0.003^{**}	0.004^{**}	0.007^{**}
	7	0.002^{**}	$<0.001^{***}$	0.032^{*}	0.038^{*}
	8	$<0.001^{***}$	$<0.001^{***}$	0.004^{**}	0.037^{*}
	9	$<0.001^{***}$	$<0.001^{***}$	0.005^{**}	0.022^{*}
	10	0.004^{**}	0.001^{**}	0.029^{*}	0.08
	11	$<0.001^{***}$	$<0.001^{***}$	$<0.001^{***}$	$<0.001^{***}$
	13	$<0.001^{***}$	$<0.001^{***}$	$<0.001^{***}$	$<0.001^{***}$
	14	$<0.001^{***}$	$<0.001^{***}$	$<0.001^{***}$	$<0.001^{***}$
	15	$<0.001^{***}$	$<0.001^{***}$	0.001^{**}	$<0.001^{***}$
R6/2 × time	4	0.524	0.344	0.689	0.4
	5	0.918	0.574	0.092	0.266
	6	0.03^{*}	0.062	0.034^{*}	0.096
	7	$<0.001^{***}$	$<0.001^{***}$	0.001^{**}	0.013^{*}
	8	0.009^{**}	$<0.001^{***}$	$<0.001^{***}$	0.005^{**}
	9	$<0.001^{***}$	$<0.001^{***}$	$<0.001^{***}$	0.004^{**}
	10	$<0.001^{***}$	$<0.001^{***}$	0.009^{**}	0.035^{*}
	11	$<0.001^{***}$	$<0.001^{***}$	$<0.001^{***}$	0.007^{**}
	13	$<0.001^{***}$	$<0.001^{***}$	$<0.001^{***}$	$<0.001^{***}$
	14	$<0.001^{***}$	$<0.001^{***}$	$<0.001^{***}$	$<0.001^{***}$
	15	$<0.001^{***}$	$<0.001^{***}$	$<0.001^{***}$	$<0.001^{***}$
tgHsp27	4	0.007^{**}	0.001^{**}	0.006^{**}	0.017^{*}
	5	0.23	0.162	0.016^{*}	0.001^{**}
	6	0.01^{*}	0.008^{**}	0.004^{**}	0.001^{**}
	7	0.08	0.036^{*}	0.006^{**}	0.003^{**}
	8	0.005^{**}	0.004^{**}	0.002^{**}	0.008^{**}
	9	0.007^{**}	0.011^{*}	0.002^{**}	0.003^{**}
	10	0.019^{*}	0.012^{*}	0.001^{**}	0.001^{**}
	11	0.003^{**}	0.006^{**}	0.006^{**}	0.006^{**}
	13	0.036^{*}	0.019^{*}	0.019^{*}	0.055
	14	0.007^{**}	0.009^{**}	0.006^{**}	0.009^{**}
	15	0.128	0.084	0.002^{**}	0.005^{**}
tgHsp27 × time	4	0.372	0.113	0.366	0.462
	5	0.677	0.277	0.227	0.276
	6	0.877	0.23	0.291	0.375
	7	0.097	0.086	0.606	0.422
	8	0.667	0.574	0.339	0.476
	9	0.835	0.569	0.417	0.382
	10	0.201	0.269	0.202	0.602
	11	0.837	0.284	0.817	0.555
	13	0.091	0.35	0.595	0.803
	14	0.349	0.113	0.392	0.697
	15	0.37	0.318	0.465	0.297
R6/2 × tgHsp27	4	0.424	0.882	0.808	0.701
	5	0.697	0.88	0.573	0.781
	6	0.932	0.766	0.546	0.796
	7	0.448	0.999	0.97	0.525
	8	0.956	0.508	0.466	0.323
	9	0.757	0.516	0.911	0.591
	10	0.746	0.706	0.5	0.772
	11	0.988	0.357	0.819	0.847
	13	0.167	0.099	0.37	0.163
	14	0.568	0.217	0.778	0.852
	15	0.921	0.443	0.5	0.641

Continued

Table 1. *Continued*

	Week	Activity	Mobility	Rearing	Centre rearing
R6/2 × tgHsp27 × time	4	0.924	0.827	0.456	0.451
	5	0.91	0.454	0.552	0.873
	6	0.043^{*}	0.435	0.396	0.291
	7	0.379	0.321	0.066	0.122
	8	0.543	0.55	0.258	0.345
	9	0.426	0.518	0.199	0.412
	10	0.451	0.254	0.895	0.683
	11	0.481	0.395	0.375	0.513
	13	0.399	0.578	0.641	0.759
	14	0.328	0.402	0.503	0.277
	15	0.423	0.788	0.439	0.253

$^{*}P < 0.05$.
$^{**}P < 0.01$.
$^{***}P < 0.001$.

in R6/2 brains, as measured by mitochondrial aconitase activity in the striatum or by protein carbonylation levels in brain.

Inclusion body formation is not influenced by Hsp27 overexpression in the brain of 3-week-old mice

Hsp27 overexpression did not modulate aggregate formation in the *in vitro* HD model (27) and, therefore, we did not expect aggregate formation to be modified in the double transgenic mice. However, overexpression of Hsp27 has been reported to assist in proteasome degradation in some paradigms (52,53) and to be a molecular chaperone without an ATPase activity, which is able to prevent inappropriate folding of proteins by maintaining its substrate in a folding-competent state (54). Recent studies in yeast showed that a related protein Hsp26 participates in a pathway which, with the action of Hsp104, can disaggregate already aggregated proteins (55,56). Therefore, we performed immunohistochemistry to assess whether *in vivo* expression of Hsp27 might have delayed the formation of aggregates in the R6/2 brain. We chose an early time point (3 weeks of age) at which aggregates are already present in a number of brain regions (8,57) to enable us to detect differences in inclusion formation. Multiple coronal sections of R6/2 and double transgenic mice were stained with the S830 N-terminal huntingtin antibody. No differences in the appearance of aggregates were noted in the hippocampus (CA1) or the striatum, between R6/2 and double transgenic mice ($n = 3$ per genotype). Therefore, Hsp27 has no effect in ameliorating R6/2 inclusion formation in brain of 3-week-old mice (Fig. 5).

Overexpressed Hsp27 can be activated by heat shock but remains inactive in the R6/2 × tgHsp27 double transgenic mice

Overall, we found that high levels of Hsp27 overexpression in R6/2 mice did not alleviate the disease phenotype. To further understand the lack of a phenotypic improvement or reduction in ROS damage, we performed native protein gel analysis to test whether in the brains of the double transgenic mice,

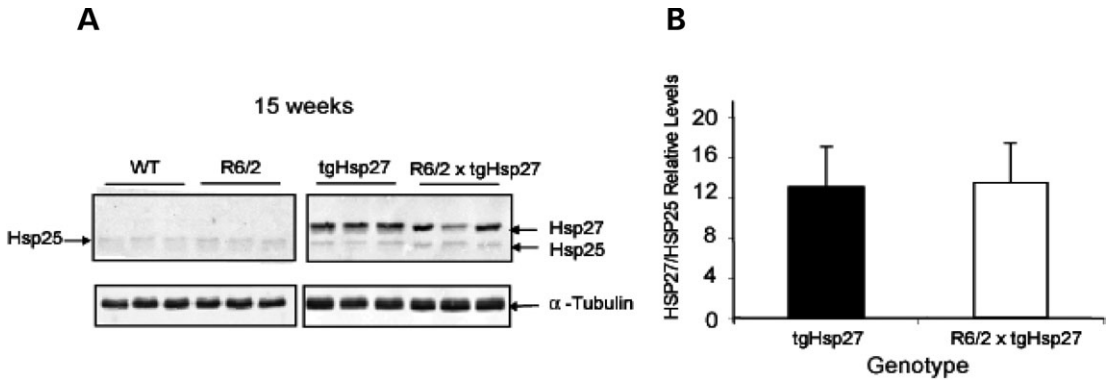

Figure 3. Hsp27 and Hsp25 expression in the brains of mice from the tgHsp27 × R6/2 genetic cross. (**A**) Representative western immunoblot of whole brain lysates from wild-type (wt), R6/2, tgHsp27 and double transgenic mice aged 15 weeks. Blots were probed with an antibody that recognizes both mouse Hsp25 and human Hsp27 and also with an anti-α-tubulin antibody to confirm equal protein loading. (**B**) Quantification of the transgene expression levels (human Hsp27) compared with the endogenous mouse Hsp25 in eight brains per genotype (four male and four female mice). Levels of Hsp27 were quantified using a phosphorimager and were expressed relatively to endogenous mouse Hsp25. Bars represent standard deviation from the mean ($n = 8$).

Hsp27 exists in the active conformation known to suppress ROS formation (58,59). Hsp27 has dynamic quaternary structure and forms either small oligomers or large complexes with non-native proteins dependent on the phosphorylation status of the protein, the physiological and developmental state of the cell and the presence of stress. Notably, large Hsp27 oligomers have an ATP-independent chaperone activity *in vitro*, absorbing heat denatured proteins onto their surface, preventing their aggregation and keeping them in a folding-competent state (59). Only large oligomers have the capacity to decrease ROS content *in vitro* and *in vivo* (58,59), and non-phosphorylatable mutant Hsp27 (which usually forms large oligomers) has been shown to protect against cell death *in vitro* (27,59) and ischemia/reperfusion injury *in vivo* (60).

Brain lysates from tgHsp27 and double transgenic mice aged 13 weeks contained only a small amount of large Hsp27 complexes, whereas the majority of the protein existed as small oligomers (the conformation devoid of chaperone activity) (Fig. 6A). Upon heat treatment (indicated by +), Hsp27 in the brain lysates rearranges into large complexes retained in the wells of the gel, indicating that it is capable of activation into the form that is known to protect from oxidative stress. This activation is dependent on the presence of heat misfolded protein substrates (Fig. 6B). As phosphorylation of Hsp27 decreases the formation of large oligomeric structures (58,59), we used Hsp27 phosphorylation-specific antibodies (to serines 15, 78 and 82) to determine whether Hsp27 is phosphorylated in the double transgenic mouse brains. We were unable to detect any evidence of phosphorylation at these sites (data not shown) and therefore conclude that Hsp27 is not inactivated by phosphorylation. Next, we attempted to determine whether Hsp27 co-localizes with the aggregation-prone mutant N-terminal huntingtin, which might be expected to be a substrate of Hsp27. However, under native gel conditions, we were not able to immunodetect the R6/2 transgene with either the S830 or 1C2 antibodies, which are routinely used to detect mutant N-terminal huntingtin in denaturing gels. Therefore, we performed co-localization and co-immunoprecipitation experiments to resolve this issue. Confocal microscopy indicated that Hsp27 does not co-localize with polyQ aggregates in the brains of double transgenic mice aged 8 weeks, as detected by the EM48 anti-huntingtin antibody or ubiquitin (data not shown). In addition, co-immunoprecipitation experiments with the S830 anti-huntingtin antibody or with Hsp27 failed to detect an interaction between Hsp27 and the exon 1 mutant huntingtin protein, although Hsp27 was co-immunoprecipitated with endogenous mouse huntingtin (Fig. 7). An interaction between wt huntingtin and Hsp27 has not previously been reported (61), but both proteins have roles in actin cytoskeleton organization (62,63). In summary, we have shown that Hsp27 in double transgenic mouse brains exists in a form which is considered to be inactive (low molecular weight oligomers), even though Hsp27 is functional when subjected to a physiological stress such as heat shock.

DISCUSSION

Overexpression of Hsp27 in a cell-based model of HD has been previously shown to suppress polyQ-mediated ROS formation and cell death (27). As ROS formation and oxidative stress are well-described features of HD (15,32,35–38,64,65) and of the R6/1 (66) and R6/2 (16,39,40) HD mouse models, we set out to determine whether overexpression of Hsp27 might prove beneficial in the R6/2 mice. Expression of Hsp27 at ~12-fold of the endogenous Hsp25 levels failed to improve the phenotype of the R6/2 mice, as assessed by weight gain, RotaRod performance, activity monitoring and grip strength. We found no suppression of oxidative damage, as judged by striatal aconitase activity or protein carbonylation; therefore, Hsp27 had not protected against detectable oxidative damage in the absence of a phenotypic improvement. Using native protein gels, we found that Hsp27 had not been activated into large oligomeric complexes at an age at which ROS damage is apparent in R6/2 mouse brains. Therefore, we suggest that the Hsp27 transprotein fails to modify the R6/2 pathology because it is not activated in this model of chronic neurodegenerative disease.

Although the Hsp27 transprotein did not show beneficial effects when overexpressed in R6/2 mice, we know that it is

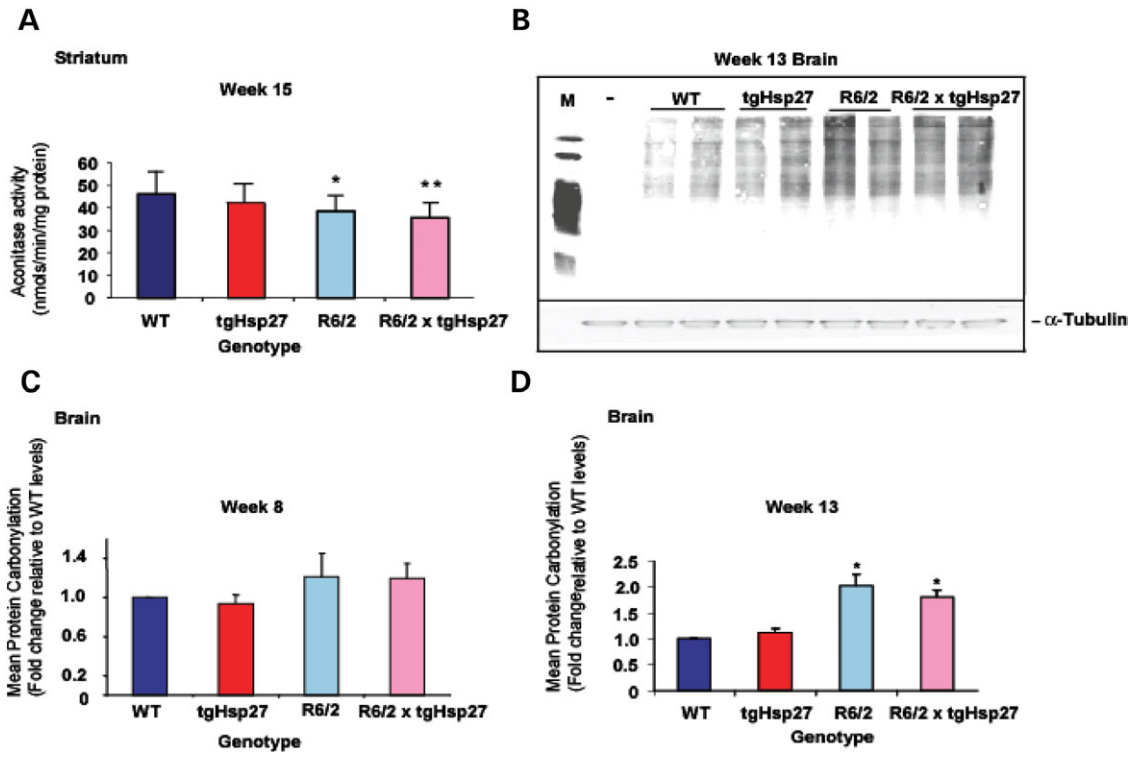

Figure 4. Hsp27 does not ameliorate free radical damage in the R6/2 brain. (**A**) Mitochondrial aconitase activity is reduced in the striata of R6/2 ($^{*}P = 0.013$) and of double transgenic mice ($^{**}P = 0.003$) when compared with wt mice at 15 weeks of age ($n = 15$ per genotype). Comparison of R6/2 and double transgenic activities shows no statistically significant difference ($P = 0.2$). Hsp27 overexpression does not confer a protective effect against ROS formation and hence oxidative damage. (**B**) Representative Oxyblot of brains from 13-week-old mice using an anti-2,4-DNP-hydrazone antibody specific for derivatized protein carbonyls in brain lysates. M, protein molecular weight standard marker and positive control for protein carbonylation; −, negative control = non-derivatized R6/2 lysate. α-Tubulin was used to confirm equal protein loading. (**C** and **D**) Quantification of protein carbonylation using Oxyblots. Total brain lysates of 8- and 13-week-old mice were derivatized ($n = 4$ and $n = 6$, respectively, per genotype). Proteins are oxidatively modified in 13-week R6/2 mice (D), and Hsp27 overexpression does not suppress this damage in the double transgenic brain. There is a significant 2-fold increase in protein carbonylation levels in both R6/2 and double transgenic brain compared with wt at week 13 ($P < 0.01$, Bonferroni multiple comparisons test), whereas no obvious differences were found between R6/2 and double transgenics and wt at week 8. WT, wild-type; R6/2 × tgHsp27, double transgenic mice.

capable of functional activation against various insults. The same tgHsp27 mice have previously been shown to be protected against kainate-induced seizures and neurodegeneration (41), ischaemia/reperfusion heart injury (42) and nerve injury (43). In all cases, these disease models are induced by an acute insult. In contrast, our data suggest that the chronic expression of an aggregation prone protein, shown to induce ROS formation, is either not capable of activating Hsp27 or maintaining this activation. Such expression also fails to activate the protective heat-shock response (21), despite causing decrease in chaperone levels (28) and loss of metastable proteins (67). It is possible that slow incremental accumulation of protein damage in misfolding disease models, as opposed to a high flux of damaged proteins in acute stress models, is either not detected by cellular stress response mechanisms or induces tolerance.

It would seem that the mouse can tolerate the long-term overexpression of Hsp27, as we did not observe overt detrimental effects, only a subtle change in exploratory activity. It is possible that a mammalian *in vivo* system cannot tolerate chronic activation of Hsp27 and the cellular protein networks equilibrate to accommodate the overexpression of this protein. Furthermore, if constitutive overexpression of Hsp27 perturbs cellular homeostasis, its inability to be protective may be generally applicable to other mouse models of neurodegenerative disease. Alternatively, we cannot rule out two other possibilities. First, as oxidative damage is not a primary pathogenic event in the R6/2 mice, other disease-related cellular dysfunctions may prevent Hsp27 activation in response to ROS. Secondly, acute stressors may not require high molecular weight oligomers (the species required to reduce ROS formation and oxidative damage), and the small molecular weight species observed in the mouse brains may be effective in these paradigms.

Although constitutive or transient overexpression of individual Hsps has been relatively successful in ameliorating disease phenotypes in cell-based, *in vitro* and invertebrate models of polyglutamine disease (19–23,68) in general, this has not translated to mammalian systems. For example, overexpression of Hsp70 had only very mild effects in mouse models of HD (28,29) and spinocerebellar ataxia type 1 (69). One reason for this may be that levels of Hdj1 and Hdj2, co-factors of Hsp70, are decreased in the R6/2 (28) and *Hdh*Q150 knock-in (70) mouse models of HD, which are important for Hsp70 chaperone activity. Similarly, overexpression of yeast Hsp104 in an HD mouse model had

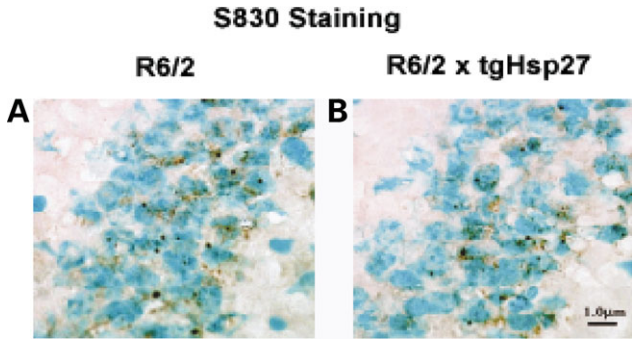

Figure 5. Hsp27 does not alter the appearance of inclusion bodies in the brain of 3-week-old R6/2 mice. Representative light microscopy images of sections of brains from mice at 3 weeks of age immunostained with the S830 N-terminal huntingtin antibody. No obvious difference in inclusion formation was detected between the CA1 region of the hippocampus of R6/2 (**A**) and double transgenic mice (**B**). Aggregate load is even less pronounced at this age in the striatum compared with the hippocampus, and again no marked difference was seen between the striatum of R6/2 and double transgenics (data not shown). Sections were counterstained with methyl green. Scale bar = 1 μm.

modest effects on inclusion formation and survival, but did not improve the overall disease phenotype (31). Hsp70 had more pronounced beneficial effects in mouse models of spinal and bulbar muscular atrophy (SBMA), but as the androgen receptor is retained in the cytoplasm in a complex with Hsp70, this may be due to a specific mechanism (71).

Alternatively, the failure of an individual chaperone overexpression to be beneficial could reflect the requirement for a finely balanced concerted action of several chaperone systems, along with the ability to up- or down-regulate their levels in response to specific cellular requirements. A better strategy might be to target the regulators of the stress-induced chaperone response, thereby coordinately inducing many chaperones with distinct and complimentary cytoprotective functions. Heat-shock factor 1 (HSF1) is a master transcriptional regulator of stress-inducible gene expression and has been shown to modify polyQ aggregation and toxicity in *C. elegans* (72). Bioactive small molecules that activate HSF1 have been reported (17). Of these, compounds that activate HSF1 by binding to Hsp90 have been shown to modify polyQ aggregation and/or toxicity in cell culture (73) and organotypic brain slice culture models (28). Two compounds, geranylgeranylacetone and 17-allylamino-17-demethoxygeldanamycin (17-AAG), have been reported to ameliorate the phenotype and/or protein aggregation in an SBMA mouse model (74,75). However, 17-AAG has poor blood brain barrier permeability (76) and does not induce the heat-shock response when administered systemically to R6/2 mice (unpublished data). The development of mice that express activated mutants of HSF1 with temporally controlled gene expression would complement pharmacological approaches and be useful for the validation of HSF1 as a therapeutic target for HD and other neurodegenerative diseases. In support of this, R6/2 mice have been crossed to mice transgenic for a constitutively active mutant HSF1, which, although not expressed in the CNS, led to increased body weight, survival and reduced polyQ inclusion formation in muscle (30).

We have recently shown that the chronic expression of mutant polyQ, an aggregation prone protein, progressively disturbs the protein-folding homeostasis (67) affecting multiple cellular pathways. Attempts to counteract pathogenic alterations by the overexpression of a single chaperone protein may be futile. All chaperones have many cellular functions and when chronically overexpressed, may have deleterious as well as beneficial consequences and cause the protein networks to further adjust to neutralize potentially damaging effects. In support of this, oxidative damage did not activate Hsp27 into large oligomeric complexes in the R6/2 mouse *in vivo*. As recent papers have highlighted the importance of oxidative damage in HD (77,78), efforts to test the effects of reducing ROS formation on HD pathogenesis should still be pursued.

MATERIALS AND METHODS

Mouse maintenance and breeding

Hemizygous R6/2 mice (5) [available from the Induced Mutant Resource, Jackson Laboratory, Bar Harbor, ME, USA, code B6CBA-TgN (HDexon1)] were bred and reared in our colony by backcrossing R6/2 males to (CBA × C57BL/6) F1 females (B6CBAF1/OlaHsd, Harlan Olac, Bicester, UK). On arrival at our facility, the TgHsp27 mice (41) were on a C57Bl/10 × CBA/Ca background and once at KCL were also maintained by backcrossing to (C57Bl/6 × CBA) F1 females. All animals had unlimited access to water and breeding chow (Special Diet Services, Witham, UK), and housing conditions and environmental enrichment were as previously described (44). In the case of mice arising from the R6/2 × TgHsp27 cross, all cages contained at least one mouse from each genotype and mice were additionally given mash consisting of powdered chow mixed with water from 12 weeks of age. Mice were subject to a 12-h light/dark cycle. Experimental procedures followed protocols according to Home Office regulations.

Genotyping

R6/2 mice were identified prior to weaning by PCR of tail-tip DNA (44), and the CAG repeat size was determined as previously described (79). TgHsp27 mice were genotyped as follows: a 25 μl reaction contained 2 μl tail-tip DNA (100 ng/μl), 0.5 μl 10 mM dNTPs, 2.5 μl Promega Buffer, 0.5 μl (of 50 μM stock) forward primer 'HCMV-F' Sequence (5′–3′): TGACGTCAATGGGTGGACTA, 0.5 μl reverse primer 'BCA-R' Sequence (5′–3′): TCACCTCGACCCATGGTAAT, 0.25 μl Promega *Taq* (5 U/μl), 1.5 μl 25 mM $MgCl_2$ and 17.25 μl ddH_2O. Cycling conditions were as follows: 94°C, 2 min, 33 × (94°C, 60 s; 50°C, 60 s; 72°C, 45 s) and 72°C, 2.5 min.

Behavioural assessment

Motor coordination was assessed using an Ugo Basile 7650 accelerating RotaRod (Linton Instrumentation, UK), modified as previously described (44). At 4 weeks of age, mice were tested on four consecutive days, with three trials per day. At 8, 11, 13 and 15 weeks of age, mice were tested on three consecutive days with three trials per day ($n = 15$ each per genotype). All mice were weighed weekly to the nearest

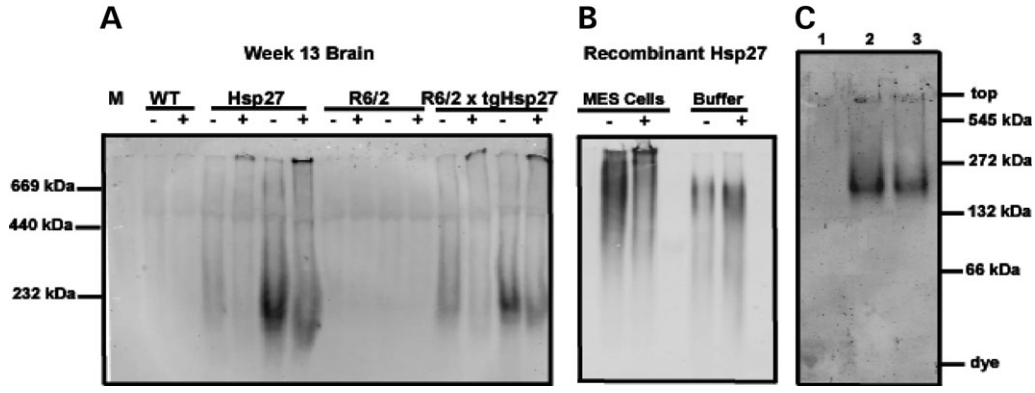

Figure 6. Hsp27 exists predominantly in an inactive low molecular weight form in brains of double transgenic mice, whereas it can be activated and form large oligomers upon heat-shock treatment. (**A**) Native protein gel analysis was performed with brain lysates of 13-week-old mice from the cross. Symbol plus indicates heat-shock treatment of lysate and minus indicates no treatment. Heat shock leads to formation of active large oligomeric complexes of Hsp27 with non-native substrates seen on the top of the gel. Prior to heat shock, tgHsp27 or double transgenic brain lysates contain predominantly low molecular weight, inactive oligomers, which shift to larger active species upon heat shock. (**B**) Mouse embryonic stem (MES) cell lysate or buffer alone was mixed with recombinant Hsp27, +/− heat shock. Note the molecular weight shift of Hsp27 upon heat shock only occurs in the presence of heat-denatured protein in the cell lysate and not in the presence of buffer alone. (**C**) Representative 7.5% gel used to precisely size the small oligomeric species. 1 = wt, 2 = tgHsp27, 3 = R6/2 × tgHsp27.

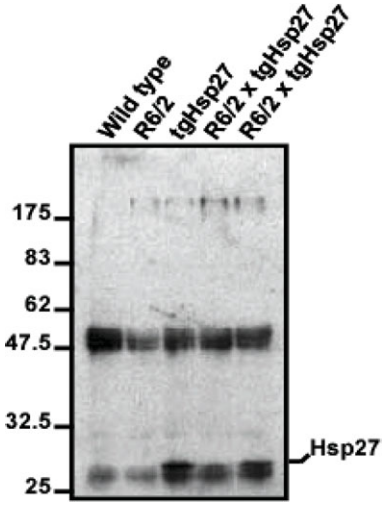

Figure 7. Co-immunoprecipitation of Hsp27 with endogenous mouse huntingtin. The S830 anti-huntingtin antibody was used to immunoprecipitate huntingtin from brain lysates, and the precipitate was fractionated on 12% SDS–PAGE gels and immunoblotted with an antibody raised against Hsp27. The non-specific bands at 55 and 25 kDa are the heavy and light IgG chains, respectively. Hsp27 has been co-immunoprecipitated with huntingtin in lysates from both the tgHsp27 and double transgenic mice. This suggests that it has co-immunoprecipitated with endogenous mouse huntingtin rather than with the R6/2 mutant exon 1 huntingtin protein.

0.1 g. Forelimb grip strength was measured once a week from 4 to 15 weeks ($n = 15$ per genotype) using a San Diego Instruments Grip Strength Meter (San Diego, CA, USA) as described (44). Exploratory, spontaneous motor activity was recorded and assessed once a week from 4 to 15 weeks of age for 60 min during the day using AM1053 activity cages, as described previously (45). Briefly, activity (total number of beam breaks in the lower level), mobility (at least two consecutive beam breaks in the lower level), rearing (number of rearing beam breaks) and centre rearing (number of rearing beam breaks which occurred away from the cage walls) were analysed. The data were collected and analysed as described previously (45).

Antibodies and western immunoblotting

Mouse brains were rapidly frozen in liquid nitrogen and stored at −80°C. Hemispheres were homogenized in 800 μl lysis buffer (50 mM Tris–HCl pH 8.0, 10% glycerol, 5 mM EDTA, 150 mM KCl) containing a cocktail of complete protease inhibitors (Boehringer Mannheim) with or without phosphatase inhibitor cocktail I and II (Sigma) using a dounce homogenizer and then sonicated for 3 × 30 s on ice (amplitude 40, Vibracell sonicator). Total protein concentration was quantified by using the bicinchoninic (BCA) Protein Assay Reagent Kit (Perbio) according to the manufacturer's instructions. Samples were mixed with gel-loading buffer and were boiled for 3 min prior to loading on a 12% SDS–PAGE gels (10–20 μg per well). Proteins were transferred onto Protran nitrocellulose membranes (Schleicher and Schuell) using a Bio-Rad transfer apparatus, and the membranes were blocked for 1 h at room temperature using 4% non-fat dried milk in phosphate-buffered saline (PBS) and then incubated with gentle agitation for 1 h at room temperature with the primary antibody diluted in PBS containing 0.5% non-fat dried milk (anti-Hsp27 goat polyclonal, Santa Cruz, 1:1000; anti-α-tubulin mouse monoclonal, Sigma, 1:2500). For chemiluminescent detection, blots were washed three times in PBS with 0.2% Tween-20 and probed with horseradish peroxidase (HRP)-linked secondary antibodies (Dako) diluted 1:3000 in 4% non-fat dried milk for 1 h at room temperature. Protein was detected by chemiluminescence (ECL kit, Amersham Biosciences) according to the manufacturer's instructions. For protein quantification, blots were probed with an Alexa 488-conjugated anti-goat secondary antibody (diluted 1:1000, Molecular Probes) and incubated for 1 h at

room temperature and then washed three times with PBS in the dark. A Typhoon 9200 PhosphorImager (Amersham Biosciences) was used for signal detection, and band intensities were calculated using ImageQuant® software (Molecular Dynamics).

The Oxyblot™ protein oxidation detection kit (S7150, Chemicon International, Temecoula, CA, USA) was used following precisely the manufacturer's instructions. Protein lysates (5 μg) were electrophoresed on 12% SDS–PAGE gels, followed by protein transfer on nitrocellulose membranes as described earlier. Protein oxidation levels were quantified using a Bio-Rad GS-800 Calibrated Densitometer using Quantity-One® Software.

Native protein gel analysis

For native protein gel electrophoresis, mouse brain hemispheres were homogenized with a pestle, proteins were extracted on ice in PELE sample buffer (20 mM Tris–HCl pH 7.4, 5 mM $MgCl_2$, 0.5% Triton X-100, 10 mM NaF, 1 mM dithiothreitol, 0.2 mM PMSF, 1 mM leupeptin, 1 mM pepstatin, 10% glycerol) and lysates centrifuged at 3000*g*. Supernatants were resolved on 7.5 or 5% acrylamide gels in the Laemmli gel system without SDS (80). Thyroglobulin (660 kDa), ferritin (440 kDa) and catalase (232 kDa) were used as molecular weight standards on 5% gels and urease h (545 kDa), urease t (272 kDa), BSA d (132 kDa) and BSA m (66 kDa) on the 7.5% gels. To transfer native proteins, the gels were incubated for 30 min at 70°C in Tris-glycine buffer (25 mM Tris, 192 mM glycine) supplemented with 0.25% SDS before electroblotting. An aliquot of 2 ng (0.1 μg/ml final concentration) of recombinant protein was used per treatment. MES cell lysate was prepared from 10 cm confluent plates as described for brain extracts. An aliquot of 20 μg of total protein was run per lane, and two mice per genotype were used. For heat-shock experiments, samples were diluted to 1 mg/ml in PELE buffer and treated at RT or 45°C for 15 min.

Co-immunoprecipitation experiments

Mouse brains were rapidly frozen in liquid nitrogen and stored at −80°C. Half brains were homogenized in 1 ml sodium phosphate buffer (20 mM NaPO4 pH 7.4, 1% SDS) with 'complete' protease inhibitors (GibcoBRL), 1 mM PMSF and 1 mM DTT. Samples were centrifuged at 2500*g* for 15 min at 4°C and sonicated for 2 × 30 s on ice (amplitude 40) (Vibracell sonicator). IP-buffer (50 mM Tris–HCl pH 7.4, 100 mM NaCl, 15 mM EDTA, 1% Triton X-100, 10% glycerol with 'complete' protease inhibitors, 1 mM PMSF, 1 mM DTT) was added to the supernatant to a final volume of 5 ml and lysates were precleared by incubation with protein A– and protein G–Sepharose agarose (Invitrogen) for 1 h at 4°C. The cleared lysate was subjected to immunoprecipitation with the addition of 1 μg of anti-S830 in a total volume of 5 ml overnight at 4°C. After incubation, protein A– and protein G–Sepharose agarose beads were added for 2 h before being washed four times with IP-buffer. The final protein agarose pellets were speed-vac dried, resuspended in two times Laemmli loading buffer and the immunoprecipitated complexes were eluted by boiling in loading buffer.

Protein samples were fractionated on 12% SDS–PAGE gels and blotted onto Protran nitrocellulose membrane (Schleicher and Schuell) by submerged transfer apparatus (Bio-Rad) in transfer buffer (25 mM Tris, 192 mM glycine and 20% v/v methanol). Membranes were blocked for 1 h at RT in 4% non-fat dried milk in PBS, 0.2% Tween-20 (PBST) and incubated with gentle agitation for 1 h at RT with anti-Hsp27 (1:1000) and mAb (Santa Cruz, Inc) in PBST with 0.5% non-fat dried milk. Blots were washed three times in PBST, probed with HRP-linked anti-goat secondary antibody (1:3000) (DAKO) in PBST with 0.5% non-fat dried milk for 1 h at RT and washed three times in PBST. Protein was detected by chemiluminescense (ECL kit, Amersham Biosciences) according to the manufacturer's instructions.

Immunohistochemical analysis

Mouse brains to be used for cryosectioning were carefully dissected and frozen in isopentane on dry ice. Coronal sections were cut at 15 μM thickness using a cryostat (Bright Instruments, Ltd, UK), fixed in 4% paraformaldehyde for 30 min and treated as previously described (81). S830 antibody (sheep polyclonal) was used at a dilution of 1:2000 and a biotinylated secondary horse anti-goat antibody was used at 1:500 (Vector laboratories). Brain sections were viewed on a Zeiss light microscope and images were captured using an Axiocam, with the help of the Zeiss Axiovision software.

Aconitase assay

Striata were carefully dissected from mouse brains, frozen in liquid nitrogen and stored at −80°C. Aconitase activity was measured as described previously (15,82).

Statistical analysis

Repeated measures GLM, one-way and two-way analysis of variance (ANOVA, for behavioural studies) and Bonferroni multiple comparisons test (Oxyblots) were performed using SPSS. The Greenhouse–Geisser correction for non-sphericity was applied to all repeated measures statistics. Student's *t*-test (protein quantification) and the Mann–Whitney *U* test (aconitase assay) were performed in Excel.

ACKNOWLEDGEMENTS

We are grateful to Emma Hockly and Jamie Tse for statistical analysis, Hilary McPhail for help with immunohistochemistry and Sunny Sunshine and Michelle Lupton for their assistance. Recombinant Hsp27 protein was purified by Dr Yoriko Atomi. This work has been generously supported by The Huntington's Disease Society of America Coalition for the Cure (to G.P.B. and R.I.M.) and the Wellcome Trust (60360; 66270).

Conflict of Interest statement. None declared.

REFERENCES

1. Bates, G.P. and Benn, C. (2000) The polyglutamine diseases. In Bates, G.P., Harper, P.S. and Jones, A.L. (eds), *Huntington's Disease*, 3rd edn. Oxford University Press, Oxford, pp. 429–472.
2. Rosas, H.D., Feigin, A.S. and Hersch, S.M. (2004) Using advances in neuroimaging to detect, understand, and monitor disease progression in Huntington's disease. *NeuroRx.*, **1**, 263–272.
3. DiFiglia, M., Sapp, E., Chase, K.O., Davies, S.W., Bates, G.P., Vonsattel, J.P. and Aronin, N. (1997) Aggregation of huntingtin in neuronal intranuclear inclusions and dystrophic neurites in brain. *Science*, **277**, 1990–1993.
4. Gutekunst, C.A., Li, S.H., Yi, H., Mulroy, J.S., Kuemmerle, S., Jones, R., Rye, D., Ferrante, R.J., Hersch, S.M. and Li, X.J. (1999) Nuclear and neuropil aggregates in Huntington's disease: relationship to neuropathology. *J. Neurosci.*, **19**, 2522–2534.
5. Mangiarini, L., Sathasivam, K., Seller, M., Cozens, B., Harper, A., Hetherington, C., Lawton, M., Trottier, Y., Lehrach, H., Davies, S.W. *et al*. (1996) Exon 1 of the HD gene with an expanded CAG repeat is sufficient to cause a progressive neurological phenotype in transgenic mice. *Cell*, **87**, 493–506.
6. Carter, R.J., Lione, L.A., Humby, T., Mangiarini, L., Mahal, A., Bates, G.P., Dunnett, S.B. and Morton, A.J. (1999) Characterization of progressive motor deficits in mice transgenic for the human Huntington's disease mutation. *J. Neurosci.*, **19**, 3248–3257.
7. Lione, L.A., Carter, R.J., Hunt, M.J., Bates, G.P., Morton, A.J. and Dunnett, S.B. (1999) Selective discrimination learning impairments in mice expressing the human Huntington's disease mutation. *J. Neurosci.*, **19**, 10428–10437.
8. Davies, S.W., Turmaine, M., Cozens, B.A., DiFiglia, M., Sharp, A.H., Ross, C.A., Scherzinger, E., Wanker, E.E., Mangiarini, L. and Bates, G.P. (1997) Formation of neuronal intranuclear inclusions underlies the neurological dysfunction in mice transgenic for the HD mutation. *Cell*, **90**, 537–548.
9. Li, H., Li, S.H., Cheng, A.L., Mangiarini, L., Bates, G.P. and Li, X.J. (1999) Ultrastructural localization and progressive formation of neuropil aggregates in Huntington's disease transgenic mice. *Hum. Mol. Genet.*, **8**, 1227–1236.
10. Stack, E.C., Kubilus, J.K., Smith, K., Cormier, K., Del Signore, S.J., Guelin, E., Ryu, H., Hersch, S.M. and Ferrante, R.J. (2005) Chronology of behavioral symptoms and neuropathological sequela in R6/2 Huntington's disease transgenic mice. *J. Comp. Neurol.*, **490**, 354–370.
11. Cha, J.H., Kosinski, C.M., Kerner, J.A., Alsdorf, S.A., Mangiarini, L., Davies, S.W., Penney, J.B., Bates, G.P. and Young, A.B. (1998) Altered brain neurotransmitter receptors in transgenic mice expressing a portion of an abnormal human huntington disease gene. *Proc. Natl Acad. Sci. USA*, **95**, 6480–6485.
12. Glass, M., Dragunow, M. and Faull, R.L. (2000) The pattern of neurodegeneration in Huntington's disease: a comparative study of cannabinoid, dopamine, adenosine and GABA(A) receptor alterations in the human basal ganglia in Huntington's disease. *Neuroscience*, **97**, 505–519.
13. Petersen, A., Gil, J., Maat-Schieman, M.L., Bjorkqvist, M., Tanila, H., Araujo, I.M., Smith, R., Popovic, N., Wierup, N., Norlen, P. *et al*. (2005) Orexin loss in Huntington's disease. *Hum. Mol. Genet.*, **14**, 39–47.
14. Strand, A.D., Aragaki, A.K., Shaw, D., Bird, T., Holton, J., Turner, C., Tapscott, S.J., Tabrizi, S.J., Schapira, A.H., Kooperberg, C. *et al*. (2005) Gene expression in Huntington's disease skeletal muscle: a potential biomarker. *Hum. Mol. Genet.*, **14**, 1863–1876.
15. Tabrizi, S.J., Cleeter, M.W., Xuereb, J., Taanman, J.W., Cooper, J.M. and Schapira, A.H. (1999) Biochemical abnormalities and excitotoxicity in Huntington's disease brain. *Ann. Neurol.*, **45**, 25–32.
16. Tabrizi, S.J., Workman, J., Hart, P.E., Mangiarini, L., Mahal, A., Bates, G., Cooper, J.M. and Schapira, A.H. (2000) Mitochondrial dysfunction and free radical damage in the Huntington R6/2 transgenic mouse. *Ann. Neurol.*, **47**, 80–86.
17. Westerheide, S.D. and Morimoto, R.I. (2005) Heat shock response modulators as therapeutic tools for diseases of protein conformation. *J. Biol. Chem.*, **280**, 33097–33100.
18. Muchowski, P.J. and Wacker, J.L. (2005) Modulation of neurodegeneration by molecular chaperones. *Nat. Rev. Neurosci.*, **6**, 11–22.
19. Muchowski, P.J., Schaffar, G., Sittler, A., Wanker, E.E., Hayer-Hartl, M.K. and Hartl, F.U. (2000) Hsp70 and hsp40 chaperones can inhibit self-assembly of polyglutamine proteins into amyloid-like fibrils. *Proc. Natl Acad. Sci. USA*, **97**, 7841–7846.
20. Krobitsch, S. and Lindquist, S. (2000) Aggregation of huntingtin in yeast varies with the length of the polyglutamine expansion and the expression of chaperone proteins. *Proc. Natl Acad. Sci. USA*, **97**, 1589–1594.
21. Satyal, S.H., Schmidt, E., Kitagawa, K., Sondheimer, N., Lindquist, S., Kramer, J.M. and Morimoto, R.I. (2000) Polyglutamine aggregates alter protein folding homeostasis in *Caenorhabditis elegans*. *Proc Natl Acad. Sci. USA*, **97**, 5750–5755.
22. Chan, H.Y., Warrick, J.M., Gray-Board, G.L., Paulson, H.L. and Bonini, N.M. (2000) Mechanisms of chaperone suppression of polyglutamine disease: selectivity, synergy and modulation of protein solubility in Drosophila. *Hum. Mol. Genet.*, **9**, 2811–2820.
23. Warrick, J.M., Chan, H.Y., Gray-Board, G.L., Chai, Y., Paulson, H.L. and Bonini, N.M. (1999) Suppression of polyglutamine-mediated neurodegeneration in Drosophila by the molecular chaperone HSP70. *Nat. Genet.*, **23**, 425–428.
24. Jana, N.R., Tanaka, M., Wang, G. and Nukina, N. (2000) Polyglutamine length-dependent interaction of Hsp40 and Hsp70 family chaperones with truncated N-terminal huntingtin: their role in suppression of aggregation and cellular toxicity. *Hum. Mol. Genet.*, **9**, 2009–2018.
25. Zhou, H., Li, S.H. and Li, X.J. (2001) Chaperone suppression of cellular toxicity of huntingtin is independent of polyglutamine aggregation. *J. Biol. Chem.*, **276**, 48417–48424.
26. Wyttenbach, A., Carmichael, J., Swartz, J., Furlong, R.A., Narain, Y., Rankin, J. and Rubinsztein, D.C. (2000) Effects of heat shock, heat shock protein 40 (HDJ-2), and proteasome inhibition on protein aggregation in cellular models of Huntington's disease. *Proc. Natl Acad. Sci. USA*, **97**, 2898–2903.
27. Wyttenbach, A., Sauvageot, O., Carmichael, J., Diaz-Latoud, C., Arrigo, A.P. and Rubinsztein, D.C. (2002) Heat shock protein 27 prevents cellular polyglutamine toxicity and suppresses the increase of reactive oxygen species caused by huntingtin. *Hum. Mol. Genet.*, **11**, 1137–1151.
28. Hay, D.G., Sathasivam, K., Tobaben, S., Stahl, B., Marber, M., Mestril, R., Mahal, A., Smith, D.L., Woodman, B. and Bates, G.P. (2004) Progressive decrease in chaperone protein levels in a mouse model of Huntington's disease and induction of stress proteins as a therapeutic approach. *Hum. Mol. Genet.*, **13**, 1389–1405.
29. Hansson, O., Nylandsted, J., Castilho, R.F., Leist, M., Jaattela, M. and Brundin, P. (2003) Overexpression of heat shock protein 70 in R6/2 Huntington's disease mice has only modest effects on disease progression. *Brain Res.*, **970**, 47–57.
30. Fujimoto, M., Takaki, E., Hayashi, T., Kitaura, Y., Tanaka, Y., Inouye, S. and Nakai, A. (2005) Active HSF1 significantly suppresses polyglutamine aggregate formation in cellular and mouse models. *J. Biol. Chem.*, **280**, 34908–34916.
31. Vacher, C., Garcia-Oroz, L. and Rubinsztein, D.C. (2005) Overexpression of yeast hsp104 reduces polyglutamine aggregation and prolongs survival of a transgenic mouse model of Huntington's disease. *Hum. Mol. Genet.*, **14**, 3425–3433.
32. Sian, J., Dexter, D.T., Lees, A.J., Daniel, S., Agid, Y., Javoy-Agid, F., Jenner, P. and Marsden, C.D. (1994) Alterations in glutathione levels in Parkinson's disease and other neurodegenerative disorders affecting basal ganglia. *Ann. Neurol.*, **36**, 348–355.
33. Saft, C., Zange, J., Andrich, J., Muller, K., Lindenberg, K., Landwehrmeyer, B., Vorgerd, M., Kraus, P.H., Przuntek, H. and Schols, L. (2005) Mitochondrial impairment in patients and asymptomatic mutation carriers of Huntington's disease. *Mov. Disord.*, **20**, 674–679.
34. Stoy, N., Mackay, G.M., Forrest, C.M., Christofides, J., Egerton, M., Stone, T.W. and Darlington, L.G. (2005) Tryptophan metabolism and oxidative stress in patients with Huntington's disease. *J. Neurochem.*, **93**, 611–623.
35. Browne, S.E., Bowling, A.C., MacGarvey, U., Baik, M.J., Berger, S.C., Muqit, M.M., Bird, E.D. and Beal, M.F. (1997) Oxidative damage and metabolic dysfunction in Huntington's disease: selective vulnerability of the basal ganglia. *Ann. Neurol.*, **41**, 646–653.
36. Mann, V.M., Cooper, J.M., Javoy-Agid, F., Agid, Y., Jenner, P. and Schapira, A.H. (1990) Mitochondrial function and parental sex effect in Huntington's disease. *Lancet*, **336**, 749.

37. Gu, M., Gash, M.T., Mann, V.M., Javoy-Agid, F., Cooper, J.M. and Schapira, A.H. (1996) Mitochondrial defect in Huntington's disease caudate nucleus. *Ann. Neurol.*, **39**, 385–389.
38. Arenas, J., Campos, Y., Ribacoba, R., Martin, M.A., Rubio, J.C., Ablanedo, P. and Cabello, A. (1998) Complex I defect in muscle from patients with Huntington's disease. *Ann. Neurol.*, **43**, 397–400.
39. Perluigi, M., Poon, H.F., Maragos, W., Pierce, W.M., Klein, J.B., Calabrese, V., Cini, C., De Marco, C. and Butterfield, D.A. (2005) Proteomic analysis of protein expression and oxidative modification in r6/2 transgenic mice: a model of Huntington disease. *Mol. Cell. Proteomics*, **4**, 1849–1861.
40. Bogdanov, M.B., Andreassen, O.A., Dedeoglu, A., Ferrante, R.J. and Beal, M.F. (2001) Increased oxidative damage to DNA in a transgenic mouse model of Huntington's disease. *J. Neurochem.*, **79**, 1246–1249.
41. Akbar, M.T., Lundberg, A.M., Liu, K., Vidyadaran, S., Wells, K.E., Dolatshad, H., Wynn, S., Wells, D.J., Latchman, D.S. and de Belleroche, J. (2003) The neuroprotective effects of heat shock protein 27 overexpression in transgenic animals against kainate-induced seizures and hippocampal cell death. *J. Biol. Chem.*, **278**, 19956–19965.
42. Efthymiou, C.A., Mocanu, M.M., de Belleroche, J., Wells, D.J., Latchman, D.S. and Yellon, D.M. (2004) Heat shock protein 27 protects the heart against myocardial infarction. *Basic Res. Cardiol.*, **99**, 392–394.
43. Sharp, P., Krishnan, M., Pullar, O., Navarrete, R., Wells, D. and de Belleroche, J. (2006) Heat shock protein 27 rescues motor neurons following nerve injury and preserves muscle function. *Exp. Neurol.*, **198**, 511–518.
44. Hockly, E., Woodman, B., Mahal, A., Lewis, C.M. and Bates, G. (2003) Standardization and statistical approaches to therapeutic trials in the R6/2 mouse. *Brain Res. Bull*, **61**, 469–479.
45. Hockly, E., Tse, J., Barker, A.L., Moolman, D.L., Beunard, J.L., Revington, A.P., Holt, K., Sunshine, S., Moffitt, H., Sathasivam, K. *et al*. (2006) Evaluation of the benzothiazole aggregation inhibitors riluzole and PGL-135 as therapeutics for Huntington's disease. *Neurobiol. Dis.*, **21**, 228–236.
46. Luthi-Carter, R., Strand, A., Peters, N.L., Solano, S.M., Hollingsworth, Z.R., Menon, A.S., Frey, A.S., Spektor, B.S., Penney, E.B., Schilling, G. *et al*. (2000) Decreased expression of striatal signaling genes in a mouse model of Huntington's disease. *Hum. Mol. Genet.*, **9**, 1259–1271.
47. Luthi-Carter, R., Hanson, S.A., Strand, A.D., Bergstrom, D.A., Chun, W., Peters, N.L., Woods, A.M., Chan, E.Y., Kooperberg, C., Krainc, D. *et al*. (2002) Dysregulation of gene expression in the R6/2 model of polyglutamine disease: parallel changes in muscle and brain. *Hum. Mol. Genet.*, **11**, 1911–1926.
48. Hodges, A., Strand, A.D., Aragaki, A.K., Kuhn, A., Sengstag, T., Hughes, G., Elliston, L.A., Hartog, C., Goldstein, D.R., Thu, D. *et al*. (2006) Regional and cellular gene expression changes in human Huntington's disease brain. *Hum. Mol. Genet.*, **15**, 965–977.
49. Regan, R.F., Chen, J. and Benvenisti-Zarom, L. (2004) Heme oxygenase-2 gene deletion attenuates oxidative stress in neurons exposed to extracellular hemin. *BMC Neurosci.*, **5**, 34.
50. Ren, Y., Liu, W., Jiang, H., Jiang, Q. and Feng, J. (2005) Selective vulnerability of dopaminergic neurons to microtubule depolymerization. *J. Biol. Chem.*, **280**, 34105–34112.
51. Lim, G.P., Chu, T., Yang, F., Beech, W., Frautschy, S.A. and Cole, G.M. (2001) The curry spice curcumin reduces oxidative damage and amyloid pathology in an Alzheimer transgenic mouse. *J. Neurosci.*, **21**, 8370–8377.
52. Shimura, H., Miura-Shimura, Y. and Kosik, K.S. (2004) Binding of tau to heat shock protein 27 leads to decreased concentration of hyperphosphorylated tau and enhanced cell survival. *J. Biol. Chem.*, **279**, 17957–17962.
53. Parcellier, A., Gurbuxani, S., Schmitt, E., Solary, E. and Garrido, C. (2003) Heat shock proteins, cellular chaperones that modulate mitochondrial cell death pathways. *Biochem. Biophys. Res. Commun.*, **304**, 505–512.
54. Ehrnsperger, M., Graber, S., Gaestel, M. and Buchner, J. (1997) Binding of non-native protein to Hsp25 during heat shock creates a reservoir of folding intermediates for reactivation. *Embo J.*, **16**, 221–229.
55. Haslbeck, M., Miess, A., Stromer, T., Walter, S. and Buchner, J. (2005) Disassembling protein aggregates in the yeast cytosol. The cooperation of Hsp26 with Ssa1 and Hsp104. *J. Biol. Chem.*, **280**, 23861–23868.
56. Cashikar, A.G., Duennwald, M. and Lindquist, S.L. (2005) A chaperone pathway in protein disaggregation. Hsp26 alters the nature of protein aggregates to facilitate reactivation by Hsp104. *J. Biol. Chem.*, **280**, 23869–23875.
57. Morton, A.J., Lagan, M.A., Skepper, J.N. and Dunnett, S.B. (2000) Progressive formation of inclusions in the striatum and hippocampus of mice transgenic for the human Huntington's disease mutation. *J. Neurocytol.*, **29**, 679–702.
58. Mehlen, P., Hickey, E., Weber, L.A. and Arrigo, A.P. (1997) Large unphosphorylated aggregates as the active form of hsp27 which controls intracellular reactive oxygen species and glutathione levels and generates a protection against TNFalpha in NIH-3T3-ras cells. *Biochem. Biophys. Res. Commun.*, **241**, 187–192.
59. Rogalla, T., Ehrnsperger, M., Preville, X., Kotlyarov, A., Lutsch, G., Ducasse, C., Paul, C., Wieske, M., Arrigo, A.P., Buchner, J. *et al*. (1999) Regulation of Hsp27 oligomerization, chaperone function, and protective activity against oxidative stress/tumor necrosis factor alpha by phosphorylation. *J. Biol. Chem.*, **274**, 18947–18956.
60. Hollander, J.M., Martin, J.L., Belke, D.D., Scott, B.T., Swanson, E., Krishnamoorthy, V. and Dillmann, W.H. (2004) Overexpression of wild-type heat shock protein 27 and a nonphosphorylatable heat shock protein 27 mutant protects against ischemia/reperfusion injury in a transgenic mouse model. *Circulation*, **110**, 3544–3552.
61. Goehler, H., Lalowski, M., Stelzl, U., Waelter, S., Stroedicke, M., Worm, U., Droege, A., Lindenberg, K.S., Knoblich, M., Haenig, C. *et al*. (2004) A protein interaction network links GIT1 an enhancer of huntingtin aggregation to Huntington's disease. *Mol. Cell*, **15**, 853–865.
62. Harjes, P. and Wanker, E.E. (2003) The hunt for huntingtin function: interaction partners tell many different stories. *Trends Biochem. Sci.*, **28**, 425–433.
63. Huot, J., Houle, F., Spitz, D.R. and Landry, J. (1996) HSP27 phosphorylation-mediated resistance against actin fragmentation and cell death induced by oxidative stress. *Cancer Res.*, **56**, 273–279.
64. Jenkins, B.G., Rosas, H.D., Chen, Y.C., Makabe, T., Myers, R., MacDonald, M., Rosen, B.R., Beal, M.F. and Koroshetz, W.J. (1998) 1H NMR spectroscopy studies of Huntington's disease: correlations with CAG repeat numbers. *Neurology*, **50**, 1357–1365.
65. del Hoyo, P., Garcia-Redondo, A., de Bustos, F., Molina, J.A., Sayed, Y., Alonso-Navarro, H., Caballero, L., Arenas, J. and Jimenez-Jimenez, F.J. (2006) Oxidative stress in skin fibroblasts cultures of patients with Huntington's disease. *Neurochem. Res.*, **31**, 1103–1109.
66. Perez-Severiano, F., Santamaria, A., Pedraza-Chaverri, J., Medina-Campos, O.N., Rios, C. and Segovia, J. (2004) Increased formation of reactive oxygen species, but no changes in glutathione peroxidase activity, in striata of mice transgenic for the Huntington's disease mutation. *Neurochem. Res.*, **29**, 729–733.
67. Gidalevitz, T., Ben-Zvi, A., Ho, K.H., Brignull, H.R. and Morimoto, R.I. (2006) Progressive disruption of cellular protein folding in models of polyglutamine diseases. *Science*, **311**, 1471–1474.
68. Chai, Y., Koppenhafer, S.L., Bonini, N.M. and Paulson, H.L. (1999) Analysis of the role of heat shock protein (Hsp) molecular chaperones in polyglutamine disease. *J. Neurosci.*, **19**, 10338–10347.
69. Cummings, C.J., Sun, Y., Opal, P., Antalffy, B., Mestril, R., Orr, H.T., Dillmann, W.H. and Zoghbi, H.Y. (2001) Over-expression of inducible HSP70 chaperone suppresses neuropathology and improves motor function in SCA1 mice. *Hum. Mol. Genet.*, **10**, 1511–1518.
70. Woodman, B., Butler, R., Landles, C., Lupton, M.K., Tse, J., Hockly, E., Moffitt, H., Sathasivam, K. and Bates, G.P. (2007) The HdhQ150/Q150 knock-in mouse model of HD and the R6/2 exon 1 model develop comparable and widespread molecular phenotypes. *Brain Res. Bull.*, **72**, 83–97.
71. Adachi, H., Katsuno, M., Minamiyama, M., Sang, C., Pagoulatos, G., Angelidis, C., Kusakabe, M., Yoshiki, A., Kobayashi, Y., Doyu, M. *et al*. (2003) Heat shock protein 70 chaperone overexpression ameliorates phenotypes of the spinal and bulbar muscular atrophy transgenic mouse model by reducing nuclear-localized mutant androgen receptor protein. *J. Neurosci.*, **23**, 2203–2211.
72. Nollen, E.A., Garcia, S.M., van Haaften, G., Kim, S., Chavez, A., Morimoto, R.I. and Plasterk, R.H. (2004) Genome-wide RNA interference screen identifies previously undescribed regulators of polyglutamine aggregation. *Proc. Natl Acad. Sci. USA*, **101**, 6403–6408.
73. Sittler, A., Lurz, R., Lueder, G., Priller, J., Hayer-Hartl, M.K., Hartl, F.U., Lehrach, H. and Wanker, E.E. (2001) Geldanamycin activates a heat shock response and inhibits huntingtin aggregation in a cell culture model of Huntington's disease. *Hum. Mol. Genet.*, **10**, 1307–1315.

74. Katsuno, M., Sang, C., Adachi, H., Minamiyama, M., Waza, M., Tanaka, F., Doyu, M. and Sobue, G. (2005) Pharmacological induction of heat-shock proteins alleviates polyglutamine-mediated motor neuron disease. *Proc. Natl Acad. Sci. USA*, **102**, 16801–16806.
75. Waza, M., Adachi, H., Katsuno, M., Minamiyama, M., Sang, C., Tanaka, F., Inukai, A., Doyu, M. and Sobue, G. (2005) 17-AAG, an Hsp90 inhibitor, ameliorates polyglutamine-mediated motor neuron degeneration. *Nat. Med.*, **11**, 1088–1095.
76. Egorin, M.J., Zuhowski, E.G., Rosen, D.M., Sentz, D.L., Covey, J.M. and Eiseman, J.L. (2001) Plasma pharmacokinetics and tissue distribution of 17-(allylamino)-17- demethoxygeldanamycin (NSC 330507) in CD2F1 mice1. *Cancer Chemother. Pharmacol.*, **47**, 291–302.
77. Cui, L., Jeong, H., Borovecki, F., Parkhurst, C.N., Tanese, N. and Krainc, D. (2006) Transcriptional repression of PGC-1alpha by mutant huntingtin leads to mitochondrial dysfunction and neurodegeneration. *Cell*, **127**, 59–69.
78. Weydt, P., Pineda, V.V., Torrence, A.E., Libby, R.T., Satterfield, T.F., Lazarowski, E.R., Gilbert, M.L., Morton, G.J., Bammler, T.K., Strand, A.D. *et al*. (2006) Thermoregulatory and metabolic defects in Huntington's disease transgenic mice implicate PGC-1alpha in Huntington's disease neurodegeneration. *Cell. Metab.*, **4**, 349–362.
79. Mangiarini, L., Sathasivam, K., Mahal, A., Mott, R., Seller, M. and Bates, G.P. (1997) Instability of highly expanded CAG repeats in mice transgenic for the Huntington's disease mutation. *Nat. Genet.*, **15**, 197–200.
80. Schagger, H., Cramer, W.A. and von Jagow, G. (1994) Analysis of molecular masses and oligomeric states of protein complexes by blue native electrophoresis and isolation of membrane protein complexes by two-dimensional native electrophoresis. *Anal. Biochem.*, **217**, 220–230.
81. Smith, D.L., Portier, R., Woodman, B., Hockly, E., Mahal, A., Klunk, W.E., Li, X.J., Wanker, E., Murray, K.D. and Bates, G.P. (2001) Inhibition of polyglutamine aggregation in R6/2 HD brain slices-complex dose-response profiles. *Neurobiol. Dis.*, **8**, 1017–1026.
82. Gardner, P.R., Nguyen, D.D. and White, C.W. (1994) Aconitase is a sensitive and critical target of oxygen poisoning in cultured mammalian cells and in rat lungs. *Proc. Natl Acad. Sci. USA*, **91**, 12248–12252.